

Homogeneous cosmologies with a cosmological constant

Martin Goliath^{1*} and George F. R. Ellis,^{2†}

¹*Department of Physics, Stockholm University, Box 6730, S-113 85 Stockholm, Sweden*

²*Department of Mathematics and Applied Mathematics, University of Cape Town, Rondebosch 7700, Cape Town, South Africa*
(July 30, 2013)

Spatially homogeneous cosmological models with a positive cosmological constant are investigated, using dynamical systems methods. We focus on the future evolution of these models. In particular, we address the question whether there are models within this class that are de Sitter-like in the future, but are tilted.

I. INTRODUCTION

This paper is concerned with the evolution of spatially homogeneous cosmological models with a cosmological constant. Several authors have addressed this problem. Stabell & Refsdal [1] investigated the Friedmann-Lemaître dust models, and a generalization of their results to general equation of state appear in [2,3]. The examination of Bianchi models with two-component fluids by Coley & Wainwright [4] contain the cosmological constant as a special case. The future evolution of Bianchi models has been considered by Wald [5], who showed that all non-type-IX Bianchi models with a positive cosmological constant isotropize. The result applies to tilted models, but it should be pointed out that the isotropization is with respect to the congruence normal to the homogeneous symmetry surfaces – not the fluid congruence. The isotropization of inhomogeneous models has been studied in a Newtonian context in [6], where some exact results were obtained. The key issue here is the degree to which such a constant (or effective constant, due to a scalar field) can lead to isotropization of the universe, and hence explain the presently observed near-isotropy. Isotropization can happen to some degree in anisotropic models without a cosmological constant [7,8], but not sufficiently to convincingly explain the degree of isotropy observed. Wald’s theorem leads credence to the claim that inflationary models can isotropize the universe as desired, but there are limits to what inflation can achieve [9]. Hence even given all these important contributions, we think it is useful to examine the issue further, specifically by giving a treatment of these models in line with the dynamical systems methods presented in e.g. the

book edited by Wainwright & Ellis [10]. We will only examine the effect of a genuine cosmological constant here; thus we do not consider proposals for a ‘varying cosmological constant’ or scalar field (or other essentially equivalent proposals). However, we believe that examination of those cases by the same dynamical systems methods, already initiated in the case of Friedmann-Lemaître geometries [11–13] and more general models [14–16], will be a worthwhile extension of what is presented here.

With the conventions we use, the field equations take the form $G_{ab} + \Lambda g_{ab} = T_{ab}$, where Λ is the cosmological constant. In this paper, it is restricted to be non-negative, $\Lambda \geq 0$, with the focus on understanding the evolution when $\Lambda > 0$. Interpreting Λ as a vacuum energy, this implies that the vacuum energy is never negative. We will additionally assume a perfect-fluid matter source with $p = (\gamma - 1)\mu$ as equation of state, where μ is the energy density, p is the pressure, and γ is a constant. Causality then requires γ to be in the interval $0 \leq \gamma \leq 2$. Furthermore, $\gamma = 0$ just corresponds to a second cosmological constant and will not be considered.

The outline of the paper is the following. In Sec. II, the Friedmann-Lemaître models are investigated. The detailed treatment of these well-known models is motivated by the fact that they contain many of the features exhibited by the more general models to be considered, and also illustrates the methods used in an example familiar to most readers. Sec. III is concerned with the Bianchi models. After some general statements about these models, we examine the simplest cases – orthogonal models of type I and II – in more detail. The section is concluded with an investigation of tilted LRS type V models, which turns out to give us reason to be cautious about the implications of the important Wald theorem [5]. In Sec. IV we consider the Kantowski-Sachs models, which turn out to have a rather rich solution structure, with a particular interesting anisotropic boundary solution. We end with some conclusions in Sec. V.

II. FRIEDMANN-LEMAÎTRE MODELS

In order to introduce the notation used and compare with earlier results, we start by investigating the Friedmann-Lemaître models. These models are homogeneous and isotropic about every point, corresponding to a six-dimensional isometry group G_6 . For a perfect fluid, the fluid motion then necessarily coincides with the congruence normal to the symmetry surfaces, and the models

*E-mail: goliath@physto.se

†E-mail: ellis@maths.uct.ac.za

are fully specified by the length scale factor $S(t)$ and a parameter $k \in \{-1, 0, 1\}$. The line element can be written

$$ds^2 = -dt^2 + S^2(t) dl_k^2, \quad (2.1)$$

where dl_k^2 is a constant-curvature three-geometry. In what follows, a dot denotes the derivative with respect to t . Defining the Hubble scalar by $H = \dot{S}/S$, the field equations and equations of motion become [17]

The Friedmann equation:

$$H^2 = \frac{1}{3}\mu - \frac{1}{6}{}^3R + \frac{1}{3}\Lambda \quad (2.2)$$

The Raychaudhuri equation:

$$\frac{\dot{S}}{S} \equiv -qH^2 = -\frac{3\gamma-2}{6}\mu + \frac{1}{3}\Lambda \quad (2.3)$$

The energy conservation equation:

$$\dot{\mu} = -3\gamma H\mu \quad (2.4)$$

Here, ${}^3R = 6k/S^2$ is the three-curvature of the symmetry surfaces and q is the deceleration parameter. Assuming $H \neq 0$, we proceed by defining dimensionless variables according to¹

$$K = \frac{{}^3R}{6H^2}, \quad \Omega = \frac{\mu}{3H^2}, \quad \Omega_\Lambda = \frac{\Lambda}{3H^2}. \quad (2.5)$$

The density parameter Ω is related to K and Ω_Λ by

The Friedmann equation:

$$\Omega = 1 + K - \Omega_\Lambda, \quad (2.6)$$

while the deceleration parameter is given by

The Raychaudhuri equation:

$$q = \frac{3\gamma-2}{2}\Omega - \Omega_\Lambda \\ = \frac{3\gamma-2}{2}(1+K) - \frac{3\gamma}{2}\Omega_\Lambda. \quad (2.7)$$

The weak energy condition together with $\Lambda \geq 0$ immediately give

$$0 \leq \Omega, \quad -1 \leq K, \quad 0 \leq \Omega_\Lambda. \quad (2.8)$$

In addition, for models with non-positive spatial curvature 3R , these quantities are compact, i.e. the range is contained in a compact interval:

$$0 \leq \Omega \leq 1, \quad -1 \leq K \leq 0, \quad 0 \leq \Omega_\Lambda \leq 1. \quad (2.9)$$

Upon introducing a new dimensionless time variable defined by $' = H^{-1} d/dt$, we obtain

$$H' = -(1+q)H, \quad (2.10)$$

$$K' = 2qK, \quad (2.11)$$

$$\Omega_\Lambda' = 2(1+q)\Omega_\Lambda. \quad (2.12)$$

Note that the H' equation is decoupled, so that we obtain a two-dimensional reduced dynamical system for K and Ω_Λ . In addition, we obtain an auxiliary equation from

The energy conservation equation:

$$\Omega' = [2q - (3\gamma - 2)]\Omega. \quad (2.13)$$

which then shows that the Friedmann equation is an integral of the Raychaudhuri equation (explicitly, the time derivative of Eq. (2.6) is the same as Eq. (2.13) in virtue of Eq. (2.11)).

A. Analysis of the dynamical system

The reduced dynamical system (2.11–2.12) has a number of invariant submanifolds:

$$\begin{array}{ll} \Omega = 0 & \text{the vacuum boundary} \\ K = 0 & \text{the flat submanifold} \\ \Omega_\Lambda = 0 & \text{the } \Lambda = 0 \text{ submanifold} \end{array}$$

Despite the appearances, $H = 0$ is *not* an invariant submanifold (As the definitions of the dimensionless variables assume $H \neq 0$, Eqs. (2.10–2.13) are not valid when $H = 0$). Equilibrium points with finite values of K and Ω_Λ lie at the intersection of these invariant submanifolds; they are

		K	Ω_Λ	Ω	q
F	the flat Friedmann solution	0	0	1	$\frac{3\gamma-2}{2}$
M	the Milne solution	-1	0	0	0
dS	the de Sitter solution	0	1	0	-1

Analyzing the stability of these equilibrium points, we find

	Eigenvalues		Stability	
			$0 < \gamma < 2/3$	$2/3 < \gamma < 2$
F	$3\gamma - 2$	3γ	saddle	source
M	$-(3\gamma - 2)$	2	source	saddle
dS	-2	-3γ	sink	sink

In addition, there might be equilibrium points associated with infinite values of K and/or Ω_Λ . This illustrates one advantage of dynamical systems with compact state space: there is no ‘infinity’ that can be difficult to analyze. In the present case, the part of state space containing models with non-positive spatial curvature ($K \leq 0$) is compact, but the region with $K > 0$ is not.

¹In [10], the curvature variable K was defined with opposite sign.

In order to compactify this region as well, we note that the Friedmann equation (2.2) can be written

$$\mu = 3H^2 + \frac{1}{2}{}^3R - \Lambda. \quad (2.14)$$

For models with ${}^3R > 0$, it is obvious that $D = \sqrt{H^2 + {}^3R/6}$ is a dominant quantity. We can thus use D , rather than H , to obtain compact variables for the $k = 1$ case:

$$Q = \frac{H}{D}, \quad \tilde{\Omega}_\Lambda = \frac{\Lambda}{3D^2}. \quad (2.15)$$

Note that the sign of Q tells if a model is in an expanding or a contracting epoch. Introducing a new time variable defined by $' = D^{-1} d/dt$, the equations become

$$D' = -\frac{3\gamma}{2}(1 - \tilde{\Omega}_\Lambda)QD, \quad (2.16)$$

$$Q' = \left[1 - \frac{3\gamma}{2}(1 - \tilde{\Omega}_\Lambda)\right](1 - Q^2), \quad (2.17)$$

$$\tilde{\Omega}'_\Lambda = 3\gamma(1 - \tilde{\Omega}_\Lambda)Q\tilde{\Omega}_\Lambda. \quad (2.18)$$

The evolution equation for D decouples, so that we obtain a reduced system in terms of Q and $\tilde{\Omega}_\Lambda$. The equilibrium points F and dS appear in this system as well. They correspond to $(Q, \tilde{\Omega}_\Lambda) = (\pm 1, 0)$ and $(Q, \tilde{\Omega}_\Lambda) = (\pm 1, 1)$, respectively. Note that there is one expanding and one contracting version of each model. For $\gamma > 2/3$ there is an additional equilibrium point E, given by

$$Q = 0, \quad \tilde{\Omega}_\Lambda = \frac{3\gamma - 2}{3\gamma}, \quad (2.19)$$

and with saddle stability. This is the Einstein static solution, for which $\dot{S} = 0, \ddot{S} = 0$. This implies $H = 0, \dot{H} = 0, \Omega \rightarrow \infty$ and $q \rightarrow \infty$, see [1]. For each value S_c of the scale factor, there is a value Λ_c of the cosmological constant that results in an Einstein static universe. More precisely,

$$\Lambda_c = \frac{3\gamma - 2}{\gamma} \frac{k}{S_c^2}, \quad (2.20)$$

so in principle, the equilibrium point E represents a one-parameter set of Einstein static universes.

The full dynamical system is obtained by matching the $K > 0$ state space with one expanding and one contracting $K < 0$ state space, see Figs. 1 and 2. The left half of the state space corresponds to expanding models, while the right half contain collapsing models. This is indicated by the subscripts of the various equilibrium points. Compact state spaces for all the Friedmann-Lemaître models were first presented in [2], and also in [18].

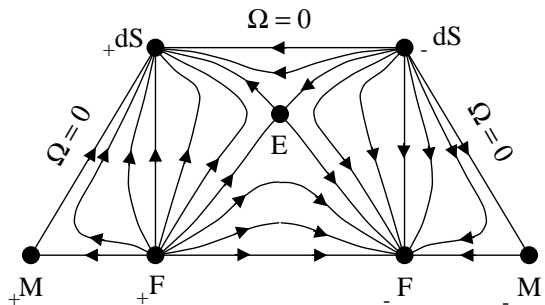


FIG. 1. State space for Friedmann-Lemaître models with $2/3 < \gamma < 2$. In the $K < 0$ regions (triangular), the vertical axis corresponds to Ω_Λ , and the horizontal axis to K . In the $K > 0$ region (rectangular), the vertical axis corresponds to $\tilde{\Omega}_\Lambda$, and the horizontal axis to Q . Subscripts on equilibrium points refer to the sign of H there.

The state space looks different, depending on whether γ is less than or greater than $2/3$.

Referring to Fig. 1, we comment on the different types of solutions for $\gamma > 2/3$. The physical domain is bounded below by the invariant submanifold $\Omega_\Lambda = 0$ and on the other sides by the invariant vacuum submanifold $\Omega = 0$. The bottom two apexes are the Milne universe (Minkowski space-time in expanding coordinates) and the top ones are the de Sitter universe. For $K < 0$ and $H > 0$, all solutions with $\Omega > 0$ and $\Lambda > 0$ expand from an initial big bang singularity $+F$ and evolve to the de Sitter model; this region is bounded by the $K = 0$ invariant submanifold (the straight line from $+F$ to $+dS$). The time reverse region occurs for $H < 0$.

For $K > 0$ and $H > 0$, the situation is more complicated [19]. Models that start out with a sufficiently small value of Λ are closed Friedmann-Lemaître models. They enter the contracting state space and recollapse to a ‘big crunch’ at $-F$. Models with large enough Λ will evolve to a de Sitter model. These are known as Lemaître models. In between these two classes, there is a separatrix orbit, corresponding to a model with $\Lambda = \Lambda_c$ and future asymptotic to the Einstein static universe. There are also models (starting off in the region with $H < 0$ and crossing to $H > 0$) that contract and expand again, without containing a singularity. The separatrix between these and the Lemaître models is the Eddington-Lemaître model, which is past asymptotic to the Einstein static universe. The vacuum orbit from $-dS$ to $+dS$ corresponds to the de Sitter universe in different slicings.

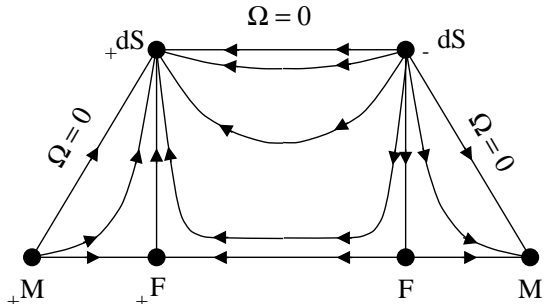


FIG. 2. State space for Friedmann-Lemaître models with $0 < \gamma < 2/3$. In the $K < 0$ regions (triangular), the vertical axis corresponds to Ω_Λ , and the horizontal axis to K . In the $K > 0$ region (rectangular), the vertical axis corresponds to $\tilde{\Omega}_\Lambda$, and the horizontal axis to Q . Subscripts on equilibrium points refer to the sign of H there.

For $\gamma < 2/3$, the situation is quite different. There is no longer an equilibrium point corresponding to the Einstein static universe. Also, the stability of the Friedmann and Milne points have changed. For $K < 0$, all solutions are asymptotic to the Milne universe in their past, and evolve to the de Sitter model in the future. For $K > 0$, there are only singularity-free contracting and re-expanding models.

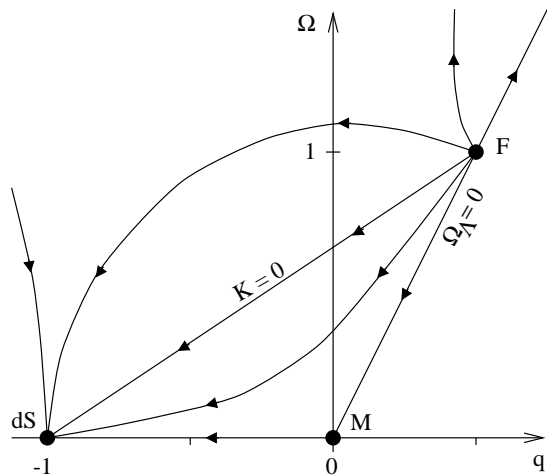
B. The (q, Ω) diagram

A useful way to illustrate cosmological models is to construct a plot of the density parameter Ω against the deceleration parameter q . This was first done by Stabell & Refsdal for the dust ($\gamma = 1$) Friedmann-Lemaître cosmologies [1], and extended to Friedmann-Lemaître models with matter and radiation by Ehlers & Rindler [20]², and to general equation of state by Madsen et al. [3].

In a (q, Ω) diagram, the different submanifolds of the Friedmann-Lemaître models are represented by straight lines as follows:

$$\begin{array}{ll} \text{vacuum} & \Omega = 0 & q \leq 0 \\ K = 0 & \Omega = \frac{2}{3\gamma}(q+1) & -1 \leq q \leq \frac{3\gamma-2}{2} \\ \Omega_\Lambda = 0 & \Omega = \frac{2}{3\gamma-2}q & \end{array}$$

We present the diagram for Friedmann-Lemaître models with $\gamma = 1$. Diagrams for other values of γ are given in [3].



²The parameter that used to be called σ [1] is the same as $\Omega/2$.

FIG. 3. (q, Ω) diagram for Friedmann-Lemaître models with $\gamma = 1$.

As the Friedmann-Lemaître models constitute a two-dimensional system, the (q, Ω) diagram will just be an alternative state space (but only representing part of the full space represented in Fig. 1). This enables us to uniquely identify equilibrium points in this diagram, in correspondence to those in Fig. 1. More explicitly, the evolution equation for Ω is given by Eq. (2.13), while that for q can be expressed as

$$q' = 2q(1+q) - \frac{3\gamma}{2}(3\gamma-2)\Omega. \quad (2.21)$$

For models represented by higher-dimensional dynamical systems, this one-to-one correspondence will in general no longer exist. The (q, Ω) diagram then represents a two-dimensional projection of the full state space, and evolution curves may consequently cross each other.

III. BIANCHI COSMOLOGIES

By dropping the assumption of isotropy, more general classes of models are obtained. The Bianchi cosmologies are models that have a three-dimensional isometry group G_3 acting on the spatial surfaces of homogeneity. There is a locally rotationally symmetric (LRS) subclass of these models, corresponding to a G_4 isometry group.

The anisotropy of these models manifests itself in a non-vanishing shear tensor $\sigma_{\alpha\beta}$. In classifying the models, one usually considers the objects $n_{\alpha\beta}$ and a_α , which describe the structure constants of the symmetry group G_3 , see e.g. [10]. The evolution equations can be obtained e.g., by appropriately specializing the equations given in [21]. Upon performing an expansion normalization in analogy with Sec. II, and with additional definitions

$$\Sigma_{\alpha\beta} \equiv \frac{\sigma_{\alpha\beta}}{H}, \quad N_{\alpha\beta} \equiv \frac{n_{\alpha\beta}}{H}, \quad A_\alpha \equiv \frac{a_\alpha}{H}, \quad (3.1)$$

we obtain

The Friedmann equation:

$$\Omega = 1 - \Sigma^2 + K - \Omega_\Lambda, \quad (3.2)$$

The Raychaudhuri equation:

$$\begin{aligned} q &= 2\Sigma^2 + \frac{3\gamma-2}{2}\Omega - \Omega_\Lambda, \\ &= \frac{3(2-\gamma)}{2}\Sigma^2 + \frac{3\gamma-2}{2}(1+K) - \frac{3\gamma}{2}\Omega_\Lambda, \end{aligned} \quad (3.3)$$

where

$$\Sigma^2 = \frac{\Sigma_{\alpha\beta}\Sigma^{\alpha\beta}}{6} \geq 0, \quad (3.4)$$

$$K = -A_\alpha A^\alpha - \frac{1}{12} [2N_{\alpha\beta}N^{\alpha\beta} - (N_\alpha^\alpha)^2]. \quad (3.5)$$

In addition to these equations, there are also evolution equations for $\Sigma_{\alpha\beta}$, etc. Here, K is the curvature parameter defined in Sec. II. The only Bianchi models for which K may be positive (i.e. ${}^3R > 0$) are of type IX. For all other Bianchi models, it follows that Ω , Σ^2 , $-K$, and Ω_Λ are compact and only take values between 0 and 1. In addition, $-1 \leq q \leq 2$. Note that this does not imply that dynamical quantities like $N_{\alpha\beta}$ need be compact.

The fluid motion need no longer be orthogonal to the surfaces of homogeneity, i.e. Bianchi models may be *tilted*. In this case, the rest spaces of an observer comoving with the fluid need not be homogeneous. When following the normal congruence, on the other hand, the fluid will no longer look perfect. Throughout this paper, kinematical quantities with respect to the normal congruence are used. A formalism for studying tilted homogeneous cosmological models has been given by King & Ellis [22].

In the orthogonal (non-tilted) case, the energy conservation equation takes the same form as in the Friedmann-Lemaître case, Eq. (2.13), ensuring that those models have an invariant vacuum ($\Omega = 0$) submanifold. In the tilted case too this will be an invariant sub-manifold (for normal fluids), as can be seen on using a comoving description.

Wald [5] has shown that Bianchi models with $K \leq 0$ will asymptotically approach a de Sitter universe in the sense that they isotropize ($\Sigma^2 \rightarrow 0$) and Λ dominates. However, as pointed out by Raychaudhuri & Modak [23], it is not guaranteed that a tilted fluid will become parallel with the normal congruence in this limit. Indeed, in Subsec. III D we will present a counter-example for which the tilt is non-vanishing for certain equations of state.

A. The (q, Ω) diagram

As discussed above, Ω and q are compact for non-type-IX models. This is useful as it leads to a compact (q, Ω) diagram, even though the state space (which usually involves more variables) may be non-compact. The boundary of the physical part of the (q, Ω) diagram can be investigated by pair-wise setting of Σ^2 , K and Ω_Λ to zero:

$$\begin{aligned} \Sigma^2 = 0 = K & & \Omega &= \frac{2}{3\gamma}(1 + q) \\ \Sigma^2 = 0 = \Omega_\Lambda & & \Omega &= \frac{2}{3\gamma-2}q \\ K = 0 = \Omega_\Lambda & & \Omega &= \frac{2}{3(2-\gamma)}(2 - q) \end{aligned}$$

The resulting diagram is a triangle with its apex at $(q, \Omega) = (\frac{3\gamma-2}{2}, 1)$. In Fig. 4, this region is depicted for $\gamma = 1$.

An important consequence of the compactness of the (q, Ω) diagram for non-type-IX models is that equilibrium points with non-zero Ω_Λ (which, by Eq. (2.12), must have $q = -1$) necessarily have $(q, \Omega) = (-1, 0)$. In addition, it follows that this uniquely specifies the variables $(\Sigma^2, K, \Omega_\Lambda)$ to be $(0, 0, 1)$.

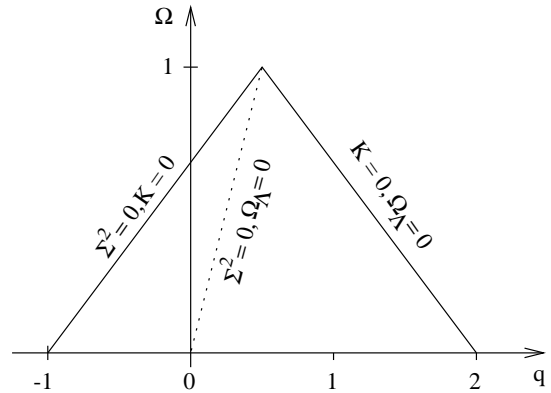


FIG. 4. Physical domain of the (q, Ω) diagram for Bianchi models with $K \leq 0$ and $\gamma = 1$.

In the case of orthogonal Bianchi models (including type IX), it is possible to show that the de Sitter point is the only new equilibrium point when extending these models from the $\Lambda = 0$ case (with the exception of possible equilibrium points at infinity for type IX), and that this point always is a sink. This follows from analyzing the general evolution equations of the orthogonal models, given in e.g. [10]. As we will see, tilted models may have additional equilibrium points.

B. Orthogonal type I

The simplest Bianchi models are the orthogonal models of type I. The shear tensor is diagonal, and consequently there are only two independent components. In expansion-normalized form, we take them to be

$$\Sigma_+ = \frac{1}{2}(\Sigma_{22} + \Sigma_{33}), \quad \Sigma_- = \frac{1}{2\sqrt{3}}(\Sigma_{22} - \Sigma_{33}). \quad (3.6)$$

With these definitions, it follows that $\Sigma^2 = \Sigma_+^2 + \Sigma_-^2$. Furthermore, $N_{\alpha\beta} = 0 = A_\alpha$, so that $K = 0$. The reduced dynamical system becomes (see e.g. [10] and Eq. (2.12))

$$\Sigma_\pm' = -(2 - q)\Sigma_\pm, \quad (3.7)$$

$$\Omega_\Lambda' = 2(1 + q)\Omega_\Lambda. \quad (3.8)$$

This three-dimensional dynamical system is compact, and has the following invariant submanifolds:

$$\begin{aligned} \Sigma_+ = 0 & & \sigma_{22} = -\sigma_{33} \\ \Sigma_- = 0 & & \text{the LRS submanifold} \\ \Omega = 0 & & \text{the vacuum boundary} \\ \Omega_\Lambda = 0 & & \text{the } \Lambda = 0 \text{ submanifold} \end{aligned}$$

Of these, the last two constitute the boundary of the state space. Apart from the equilibrium points in the $\Lambda = 0$ submanifold (see, e.g. [10]), the de Sitter (dS) point is the only additional equilibrium point, as expected.

		Σ^2	Ω_Λ	Stability
F	Friedmann	0	0	saddle
K	Kasner circle	1	0	source
dS	de Sitter	0	1	sink

The state space is depicted in Fig. 5.

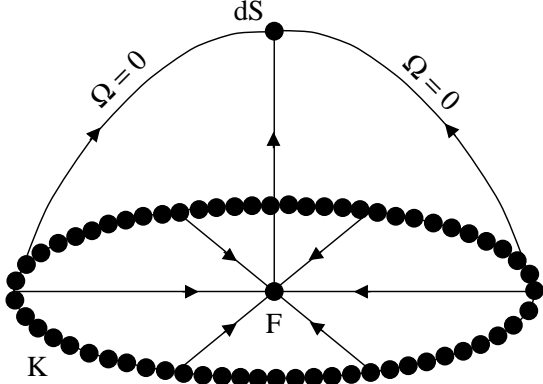


FIG. 5. State space for orthogonal Bianchi models of type I. The vertical axis corresponds to Ω_Λ , and the horizontal planes are spanned by Σ_+ and Σ_- . The ‘bottom’ is the $\Omega_\Lambda = 0$ submanifold.

As the dynamical system is invariant under rotations around the F-dS axis, there will be a one-to-one correspondence between the state space and the (q, Ω) diagram (Fig. 6), even though the system is three-dimensional. Note that the Kasner circle is represented by a single point in that diagram.

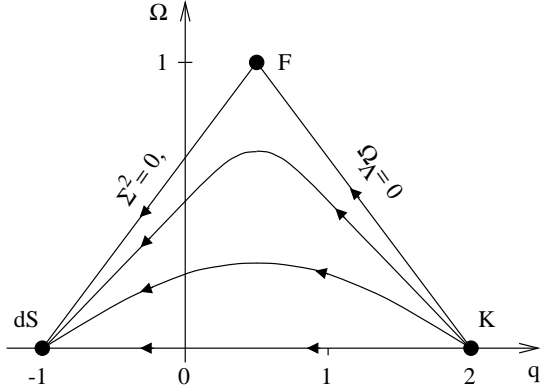


FIG. 6. The (q, Ω) diagram for orthogonal Bianchi models of type I with $\gamma = 1$.

C. Orthogonal type II

This model also has the shear fully specified by Σ_+ and Σ_- , defined in Eq. (3.6). In addition $A_\alpha = 0$, and there is only one non-zero component of $N_{\alpha\beta}$. We will take it to be $N \equiv N_{11} \geq 0$. It follows from Eq. (3.5) that $K = -N^2/12$. The reduced dynamical system becomes (see e.g. [24,10] and Eq. (2.12))

$$\Sigma_+' = -(2 - q)\Sigma_+ + N^2/3, \quad (3.9)$$

$$\Sigma_-' = -(2 - q)\Sigma_-, \quad (3.10)$$

$$N' = (q - 4\Sigma_+)N, \quad (3.11)$$

$$\Omega_\Lambda' = 2(1 + q)\Omega_\Lambda. \quad (3.12)$$

Again, we end up with a compact state space. The invariant submanifolds are the following:

- $N = 0$ the type I submanifold
- $\Sigma_- = 0$ the LRS submanifold
- $\Omega = 0$ the vacuum boundary
- $\Omega_\Lambda = 0$ the $\Lambda = 0$ submanifold

There is one new equilibrium point when $\gamma > 2/3$: P_1^+ , described in e.g. [10]. Although a sink in the $\Lambda = 0$ submanifold, the P_1^+ point is a saddle in the full state space. The future attractor of the system still is the dS point, in correspondence with the discussion of this point in Subsec. III A. As the state space is four-dimensional and hard to visualize, we present a state space diagram for the LRS submanifold (Fig. 7). Note that this is a special case of the two-fluid models studied in [4].

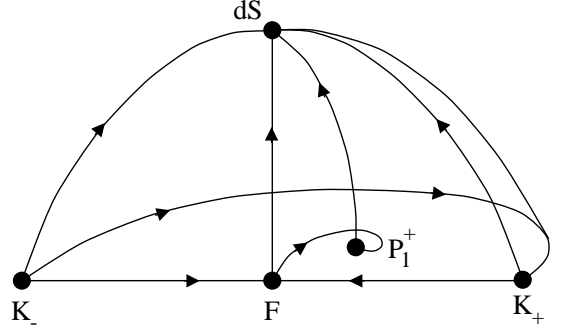


FIG. 7. State space for orthogonal LRS Bianchi models of type II. The vertical axis corresponds to Ω_Λ , the line between K_- and K_+ is the Σ_+ axis, and the third direction is the N axis. The ‘bottom’ is the $\Omega_\Lambda = 0$ submanifold.

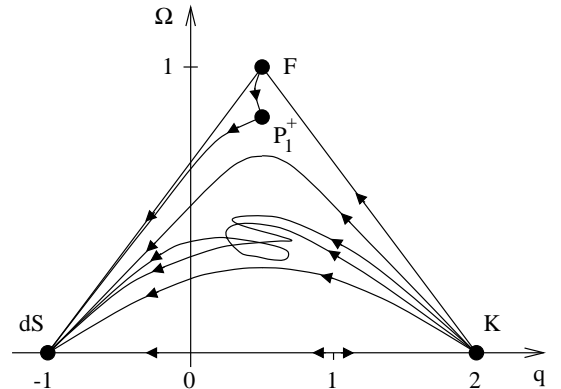


FIG. 8. The (q, Ω) diagram for orthogonal LRS Bianchi models of type II with $\gamma = 1$.

To obtain the corresponding (q, Ω) diagram, we have studied the orthogonal LRS type II system numerically. Some sample curves are displayed in Fig. 8. Note that the equilibrium points still can be uniquely identified,

except the two Kasner points, which both correspond to the point $(2, 0)$. The curves that have a cusp or loop correspond to state space orbits that start at K_- and approach K_+ , from which they are subsequently repelled. The vacuum orbit between K_- and K_+ has q going from 2 to 0 and back to 2 again, hence the arrows in both directions on the positive part of the q -axis.

D. Tilted LRS type V

So far, we have only provided examples of models where the fluid flow is orthogonal to the surfaces of homogeneity. However, as discussed above, Bianchi models allow for a fluid flow that is tilted with respect to the normal congruence of the symmetry surfaces. Here, we will consider tilted LRS type V models. The $\Lambda = 0$ case of these models were studied in [25]. Our starting point will be the dynamical systems analysis of tilted type V models by Hewitt & Wainwright [26], which we will extend to the $\Lambda \neq 0$ case.

As previously pointed out, the kinematical quantities associated with the normal congruence n^a of the spatial symmetry surfaces, rather than the fluid flow u^a , are used as variables. Following King & Ellis [22], a tilt variable v is introduced, so that in an orthonormal frame where $n^a = (1, 0, 0, 0)$, we have

$$u^a = \frac{1}{\sqrt{1-v^2}}(1, v, 0, 0). \quad (3.13)$$

In the LRS case, the normal congruence is fully described by its expansion θ and one shear variable, taken to be $\sigma = 3[\sigma_{22} + \sigma_{33}]/2$. In addition, the structure constants are fully described by one variable, which is taken to be a_1 . The field equations and conservation equations now give a constrained dynamical system in the variables (θ, σ, a_1, v) . The relations between (θ, σ) and the kinematic quantities of the fluid flow have been given in [26]. By introducing dimensionless variables $\Sigma = \sigma/\theta$ and $A = 3a_1/\theta$, and a new dimensionless time variable $' = 3/\theta d/dt$, the θ equation decouples, and a reduced dynamical system with compact state space is obtained [26]. A cosmological constant is included by introducing an additional variable $\Omega_\Lambda = 3\Lambda/\theta^2$. The equations become

The Friedmann equation:

$$\Omega = \frac{3\mu_n}{\theta^2} = 1 - \Sigma^2 - A^2 - \Omega_\Lambda, \quad (3.14)$$

where μ_n is the energy density as seen by an observer moving with the normal congruence.

The Raychaudhuri equation:

$$\theta' = -(1+q)\theta, \quad (3.15)$$

$$q = 2 - 2A^2 - 3\Omega_\Lambda - \frac{3(2-\gamma) + (5\gamma-6)v^2}{2[1+(\gamma-1)v^2]}\Omega, \quad (3.16)$$

Reduced system:

$$\Sigma' = -(2-q-2Av)\Sigma, \quad (3.17)$$

$$A' = (q+2\Sigma)A, \quad (3.18)$$

$$v' = \frac{v(1-v^2)}{1-(\gamma-1)v^2} [2\Sigma + 3\gamma - 4 - 2(\gamma-1)Av], \quad (3.19)$$

$$\Omega_\Lambda' = 2(1+q)\Omega_\Lambda, \quad (3.20)$$

Constraint:

$$\gamma v \Omega + 2[1+(\gamma-1)v^2]A\Sigma = 0, \quad (3.21)$$

There is also an auxiliary equation for Ω' that shows that $\Omega = 0$ is an invariant submanifold. Note that the curvature variable used elsewhere in this paper is given by $K = -A^2$. We assume that $A \geq 0$, without loss of generality.

The system has a number of invariant submanifolds:

$\Sigma = 0$	$\sigma_{22} = -\sigma_{33}$
$A = 0$	the LRS type I submanifold
$v = 0$	the orthogonal submanifold
$v = \pm 1$	extreme tilt
$\Omega = 0$	the vacuum boundary
$\Omega_\Lambda = 0$	the $\Lambda = 0$ submanifold

Note that $v = 0$ implies that either $\Sigma = 0$ or $A = 0$. This follows from the constraint, Eq. (3.21). The former case results in the same equations as for the Friedmann-Lemaître models with $K \leq 0$.

The following equilibrium points can be identified:

		Σ	A	v	Ω_Λ
F	flat Friedmann	0	0	0	0
M	Milne	0	1	0	0
M^\pm	—”—	0	1	± 1	0
\tilde{M}	—”—	0	1	$\frac{3\gamma-4}{2(\gamma-1)}$	0
K_\pm	Kasner	± 1	0	0	0
K_\mp	—”—	± 1	0	∓ 1	0
dS	de Sitter	0	0	0	1
dS^\pm	—”—	0	0	± 1	1

Note that all these equilibrium points except F are on the vacuum boundary (This does not mean that μ need to be vanishing. Indeed, the Kasner points have $\mu \rightarrow \infty$, $\theta \rightarrow \infty$). In addition, there is a line \mathcal{H} of equilibrium points at $v = 1$ for which $A = 1 + \Sigma$, $-1 < \Sigma < 0$. Furthermore, there are two equilibrium points K_\pm^\pm for which $\Sigma = v = \pm 1$. As they are not part of the closure of the interior of state space, we need not consider them.

Doing a stability analysis, most of the equilibrium points are found to be saddles. The exceptions are the following:

	$0 < \gamma < 2/3$	$2/3 < \gamma < 4/3$	$4/3 < \gamma < 2$
M^+	source	source	source
K_+	saddle	source	source
K_+^-	source	saddle	saddle
K_-^+	source	source	source
dS	sink	sink	saddle
dS^\pm	saddle	saddle	sink
\mathcal{H}	source	source	source

Thus, it is found that there are *three* equilibrium points for which $\Omega_\Lambda \neq 0$: the de Sitter point dS , and two de Sitter points dS^\pm with extreme tilt ($v = \pm 1$). The vacuum orbits between these points and dS correspond to the de Sitter model in different slicings, i.e. with different values of v . When $\gamma > 4/3$, it turns out that dS is a saddle point, while dS^\pm become sinks. The threshold value $\gamma = 4/3$ is particularly interesting, as $\Omega_\Lambda = 1$ then implies $v' = 0$ for *any* value of v . In other words, for each value of the tilt variable v , there is a de Sitter equilibrium point. Figs. 9–11 depict the state space of these models for various γ -intervals. As this state space represents a dynamical system with four variables and a constraint, it is not always possible to unambiguously identify a direction with a certain variable. Still, the vertical direction corresponds to Ω_Λ .

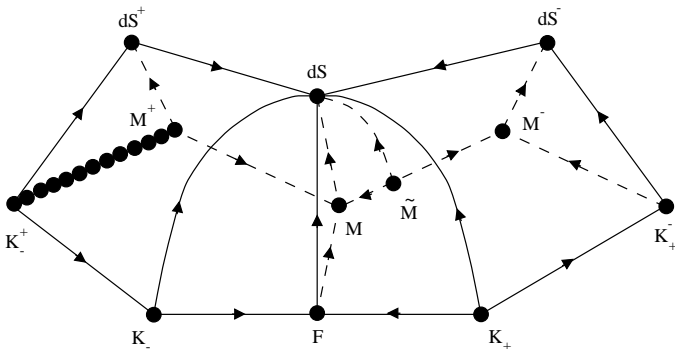


FIG. 9. State space for tilted LRS Bianchi models of type V with $6/5 < \gamma < 4/3$. The vertical axis corresponds to Ω_Λ . The ‘bottom’ is the $\Omega_\Lambda = 0$ submanifold.

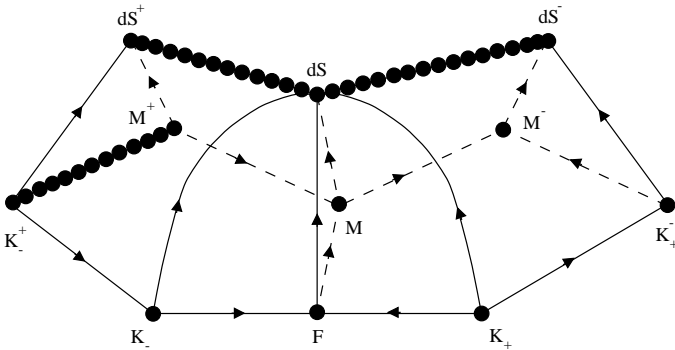


FIG. 10. State space for tilted LRS Bianchi models of type V with $\gamma = 4/3$. The vertical axis corresponds to Ω_Λ . The ‘bottom’ is the $\Omega_\Lambda = 0$ submanifold.

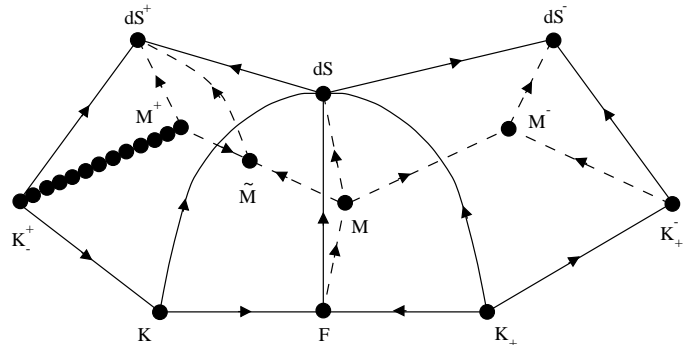


FIG. 11. State space for tilted LRS Bianchi models of type V with $4/3 < \gamma < 2$. The vertical axis corresponds to Ω_Λ . The ‘bottom’ is the $\Omega_\Lambda = 0$ submanifold.

Thus generically the space-time becomes de Sitter-like, in accordance with the Wald theorem, but the tilt does not die away, in accordance with the cautionary note given by Raychaudhuri and Modak; hence at first glance, isotropization of the cosmology does not occur. However one must be cautious about this: de Sitter space-time can be described in terms of many congruences of curves, because there is no preferred congruence in a space-time of constant curvature (cf. [27]); on switching to a description based on the family of spacelike surfaces orthogonal to the flow lines (highly tilted relative to the original surfaces of constant time), the space-time may again appear isotropic at late times. But if so, that is not the end of the story: the question then occurs as to what happens on reheating at the end of any inflationary epoch that may be represented by this model: does the matter in the universe remember the original reference frame? If it does, then after reheating the universe may be highly anisotropic; but if it does not, then the matter may still emerge from reheating in an anisotropic way precisely because there is no preferred reference frame in a de Sitter space-time, so the matter does not know what reference frame to choose after reheating (see [28] for a discussion).

A further complication is that it may be possible to extend beyond the apparent limiting point to a region with timelike symmetries, as happens in the solutions discussed by Collins and Ellis (note that this is not a problem for the $\gamma = 4/3$ de Sitter-like solutions with non-extreme tilt); this needs careful investigation.³

Thus the implications are unclear; they certainly deserve further investigation, in particular because tilt is the generic case.

³The flow lines cannot continue across a surface $\Omega = 0$, as this is an invariant surface of the flow, but one may be able to continue the family of solutions beyond by analytic continuation.

IV. KANTOWSKI-SACHS COSMOLOGIES

In order to make the discussion of spatially homogeneous cosmologies complete, we examine the Kantowski-Sachs cosmologies, which are models with an isometry group G_4 whose G_3 subgroup acts multiply transitively on two-dimensional spherically symmetric surfaces. The Einstein tensor is diagonal, showing that these models cannot be tilted. The global structure of these models has been studied by Collins [29], and a dynamical system with compact state space has been obtained [30,31]. Here, we will extend this dynamical system to include a cosmological constant.

The Friedmann equation for Kantowski-Sachs models can be written

$$\mu = 3H^2 - 3\sigma_+^2 + {}^3R/2 - \Lambda, \quad (4.1)$$

where ${}^3R > 0$ and $\sigma_+ = (\sigma_{22} + \sigma_{33})/2$. Following [31], we assume $\mu \geq 0$ and identify the dominant quantity $D = \sqrt{H^2 + {}^3R/6}$. We are now able to obtain a compact state space by normalizing with D , rather than H . Thus, we define compact variables $Q_0 = H/D$, $Q_+ = \sigma_+/D$ and $\tilde{\Omega}_\Lambda = \Lambda/3D^2$. In addition, a new dimensionless time $t' = D^{-1} d/dt$ is introduced. The dynamical system becomes *The Friedmann equation:*

$$\Omega_D = \frac{\mu}{3D^2} = 1 - Q_+^2 - \tilde{\Omega}_\Lambda, \quad (4.2)$$

Decoupled equation:

$$D' = - \left[Q_+ + Q_0 \left(3Q_+^2 - Q_0 Q_+ + \frac{3\gamma}{2} \Omega_D \right) \right] D, \quad (4.3)$$

Reduced system:

$$Q_0' = (1 - Q_0^2) \left(1 + Q_0 Q_+ - 3Q_+^2 - \frac{3\gamma}{2} \Omega_D \right), \quad (4.4)$$

$$Q_+' = -(1 - Q_+^2) (1 - Q_0^2 + 3Q_0 Q_+) + \frac{3\gamma}{2} \Omega_D Q_0 Q_+, \quad (4.5)$$

$$\tilde{\Omega}_\Lambda' = -2 \frac{D'}{D} \tilde{\Omega}_\Lambda, \quad (4.6)$$

In addition, we also obtain $\Omega_D' = -(3\gamma Q_0 + 2 \frac{D'}{D}) \Omega_D$, showing $\Omega_D = 0$ to be an invariant submanifold. Some other invariant submanifolds are also found. To summarize, we have:

$$\begin{aligned} Q_0 = \pm 1 & \quad \text{flat } ({}^3R = 0) \text{ submanifolds} \\ \Omega_D = 0 & \quad \text{the vacuum boundary} \\ \tilde{\Omega}_\Lambda = 0 & \quad \text{the } \Lambda = 0 \text{ submanifold} \end{aligned}$$

The system has a number of equilibrium points:

		Q_0	Q_+	$\tilde{\Omega}_\Lambda$	stability
$\pm F$	flat Friedmann	± 1	0	0	saddle
$+K_\pm$	Kasner	1	± 1	0	source
$-K_\pm$	—”—	-1	± 1	0	sink
$+dS$	de Sitter	1	0	1	sink
$-dS$	—”—	-1	0	1	source
$\pm X$	see text	$\pm 1/2$	$\mp 1/2$	$3/4$	saddle

All these are points on the vacuum boundary, except $\pm F$ for which $\Omega_D = 1$. It should be pointed out that although $\pm F$ are saddles in the whole interval $0 < \gamma < 2$, the stability is changed at $\gamma = 2/3$. We will only present state space diagrams for the case $2/3 < \gamma < 2$.

The $+X$ point corresponds to an exact solution with $H = -\sigma_+ = \frac{1}{3}\sqrt{\Lambda}$, and line element

$$ds^2 = -dt^2 + e^{2\sqrt{\Lambda}t} dx^2 + dy^2 + dz^2. \quad (4.7)$$

This can be interpreted as a space-time where the shear exactly counter-balances the expansion in all but one spatial direction. This solution has a ‘pancake’ singularity in the past. The contracting analogue of this solution is associated with $-X$. The solutions corresponding to these points have been discussed in [32–35].

Thus, the state space (Fig. 12) exhibits many similarities with the $K > 0$ Friedmann-Lemaître models: the state space is divided into two halves, one of which corresponds to an expanding epoch ($Q_0 > 0$) and one where the models are contracting ($Q_0 < 0$). In each half, there is a point corresponding to the de Sitter solution. The points $\pm X$ have a role similar to the Einstein static point in the Friedmann-Lemaître state space. Indeed, just as in that case, the Kantowski-Sachs state space also contains models that contract and expand again without ever being singular. Also, note the surfaces of separatrix orbits associated with the Friedmann points $\pm F$.

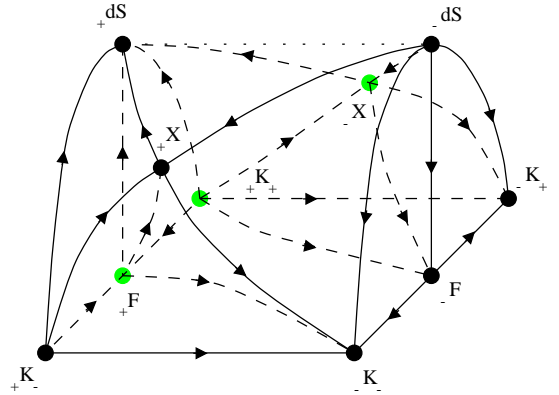


FIG. 12. State space for Kantowski-Sachs models with $2/3 < \gamma < 2$. The points $\pm X$ are located on the vacuum boundary. The vertical axis corresponds to $\tilde{\Omega}_\Lambda$, the line from $+K_-$ to $-K_-$ is the Q_0 axis, and the third axis corresponds to Q_+ . The ‘bottom’ is the $\tilde{\Omega}_\Lambda = 0$ submanifold. The equilibrium points that have been drawn in shaded color are ‘screened’.

To facilitate an easier understanding of the Kantowski-Sachs state space (Fig. 12), we present a picture of the $\tilde{\Omega}_\Lambda = 0$ submanifold (Fig. 13). This state space was first given in [30].

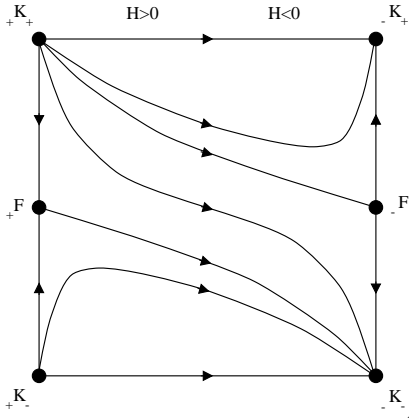


FIG. 13. State space for the Kantowski-Sachs $\tilde{\Omega}_\Lambda = 0$ submanifold with $2/3 < \gamma < 2$. The horizontal axis corresponds to Q_0 , and the vertical axis to Q_+ .

V. CONCLUSIONS

We have examined the evolution of various homogeneous cosmological models. The inclusion of a cosmological constant greatly affects the late-time behavior. For example, most Bianchi models will evolve to a de Sitter universe and isotropize, as pointed out by Wald [5]. The models presented here confirm the broad picture presented by Wald of a positive cosmological constant leading to isotropization in the orthogonal case, but leave it open in the more general tilted case. More precisely, there are models for which the tilt does not vanish at late times. To an observer moving with the fluid, this model will not seem to isotropize. These models may appear isotropic in another frame at late times, but whether that is in fact true or not is an open question. Tilted models deserve more investigation, as does the case of a realistic scalar field representation (the investigation here can represent a model including a slow-rolling scalar field, but not one where the dynamics of the scalar field is more interesting).

ACKNOWLEDGMENTS

The authors would like to thank Alan Coley, Ulf Nilsson, Claes Uggla and John Wainwright for helpful discussions. MG was supported by a grant from Wallenbergstiftelsens jubileumsfond.

[1] R. Stabell and S. Refsdal, *Mon. Not. R. Astron. Soc.* **132**, 279 (1966).
[2] M. S. Madsen and G. F. R. Ellis, *Mon. Not. R. Astron. Soc.* **234**, 67 (1988).

[3] M. S. Madsen, J. P. Mimoso, J. A. Butcher, and G. F. R. Ellis, *Phys. Rev. D* **46**, 1399 (1992).
[4] A. A. Coley and J. Wainwright, *Class. Quant. Grav.* **9**, 651 (1992).
[5] R. M. Wald, *Phys. Rev. D* **28**, 2118 (1983).
[6] U. Brauer, A. Rendall, and O. Reula, *Class. Quant. Grav.* **11**, 2283 (1994).
[7] C. W. Misner, *Phys. Rev. Lett.* **22**, 1071 (1969).
[8] J. Wainwright, G. F. R. Ellis, and M. Hancock, *Class. Quant. Grav.* **15**, 331 (1998).
[9] A. Rothman and G. F. R. Ellis, *Phys. Lett. B* **180**, 19 (1986).
[10] J. Wainwright and G. F. R. Ellis, *Dynamical systems in cosmology* (Cambridge University Press, Cambridge, 1997).
[11] V. A. Belinskii, L. P. Grischuk, Ya. B. Zel'dovich, and I. M. Khalatnikov, *Sov. Phys. JETP* **62**, 195 (1985).
[12] V. A. Belinskii, H. Ishihara, I. M. Khalatnikov, and H. Sato, *Prog. Theoret. Phys.* **79**, 676 (1988).
[13] E. J. Copeland, A. R. Liddle, and D. Wands, *Phys. Rev. D* **57**, 4686 (1998).
[14] R. J. van den Hoogen, A. A. Coley, and J. Ibáñez, *Phys. Rev. D* **55**, 5215 (1997).
[15] A. A. Coley, J. Ibáñez, and R. J. van den Hoogen, *J. Math. Phys.* **38**, 5256 (1997).
[16] A. P. Billyard, A. A. Coley, and R. J. van den Hoogen, *Phys. Rev. D* **58**, 123501 (1998).
[17] S. W. Hawking and G. F. R. Ellis, *The large scale structure of space-time* (Cambridge University Press, Cambridge, 1973).
[18] J. Wainwright, "Relativistic Cosmology", in *Proceedings of the 46th Scottish Universities Summer School in Physics*, eds. G. Hall and J. Pulman, Institute of Physics Publishing, Bristol, 1996.
[19] H. P. Robertson, *Rev. Mod. Phys.* **5**, 62 (1933).
[20] J. Ehlers and W. Rindler, *Mon. Not. R. Astron. Soc.* **238**, 503 (1989).
[21] H. van Elst and C. Uggla, *Class. Quant. Grav.* **14**, 2673 (1997).
[22] A. R. King and G. F. R. Ellis, *Commun. Math. Phys.* **31**, 209 (1973).
[23] A. K. Raychaudhuri and B. Modak, *Class. Quant. Grav.* **5**, 225 (1988).
[24] C. Uggla, *Class. Quant. Grav.* **6**, 383 (1989).
[25] C. B. Collins and G. F. R. Ellis, *Phys. Rep.* **56**, 65 (1979).
[26] C. G. Hewitt and J. Wainwright, *Phys. Rev. D* **46**, 4242 (1992).
[27] E. Schrödinger, *Space-Time Structure* (Cambridge University Press, Cambridge, 1961).
[28] P. Aninos, R. A. Matzner, and T. Rothman, *Phys. Rev. D* **43**, 3821 (1991).
[29] C. B. Collins, *J. Math. Phys.* **18**, 2116 (1977).
[30] C. Uggla and H. von zur Mühlen, *Class. Quant. Grav.* **7**, 1365 (1990).
[31] M. Goliath, U. S. Nilsson, and C. Uggla, *Class. Quant. Grav.* **15**, 167 (1998).
[32] E. Weber, *J. Math. Phys.* **25**, 3279 (1984).
[33] E. Weber, *J. Math. Phys.* **26**, 1308 (1985).
[34] Ø. Grøn and E. Eriksen, *Phys. Lett. A* **121**, 217 (1987).
[35] P. Varghas Moniz, *Phys. Rev. D* **47**, 4315 (1993).